Available online at www.sciencedirect.com
SCIENCE DIRECT®
ELSEVIER
Physica D 201 (2005) 27–44
PHYSICA D
www.elsevier.com/locate/physd

Vanishing twist in the Hamiltonian Hopf bifurcation

H.R. Dullin[a,b,*], A.V. Ivanov[a]

[a] *Department of Mathematical Sciences, Loughborough University, LE11 3TU, UK*
[b] *Fachbereich 1, Physik, Universität Bremen, 28334 Bremen, Germany*

Received 21 May 2003; received in revised form 10 December 2004; accepted 20 December 2004
Communicated by C.K.R.T. Jones

Abstract

The Hamiltonian Hopf bifurcation has an integrable normal form that describes the passage of the eigenvalues of an equilibrium through the $1:-1$ resonance. At the bifurcation the pure imaginary eigenvalues of the elliptic equilibrium turn into a complex quadruplet of eigenvalues and the equilibrium becomes a linearly unstable focus–focus point. We explicitly calculate the frequency (ratio) map of the integrable normal form, in particular we obtain the rotation number as a function on the image of the energy–momentum map in the case where the fibres are compact. We prove that the isoenergetic non-degeneracy condition of the KAM theorem is violated on a curve passing through the focus–focus point in the image of the energy–momentum map. This is equivalent to the vanishing of twist in a Poincaré map for each energy close to that of the focus–focus point. In addition we show that in a family of periodic orbits (the non-linear normal modes) the twist also vanishes. These results imply the existence of all the unusual dynamical phenomena associated with non-twist maps near the Hamiltonian Hopf bifurcation.

Keywords: Hamiltonian Hopf bifurcation; KAM; Isoenergetic non-degeneracy; Vanishing twist; Elliptic integrals

1. Introduction

Understanding the dynamics of a Hamiltonian system near equilibrium points is of fundamental importance. In the elliptic case, the eigenvalues of the linearization are pure imaginary, $\lambda_j = \pm i\omega_j$, $j = 1, \ldots, n$, where n is the number of degrees of freedom, which will be 2 in the following. By the Lyapunov Centre theorem the n normal modes of the linear approximation persist in the non-linear system when the eigenvalues are non-resonant. The resonant cases were much more recently treated [22,17,6,16]. In some sense, the most exceptional resonance is the so called $1:-1$ resonance, in which the quadratic part H_2 of the Hamiltonian H has degenerate eigenvalues and is not definite, $2H_2 = \omega(p_x^2 + x^2) - \omega(p_y^2 + y^2)$. The unfolding of the normal form gives a family of Hamiltonian

* Corresponding author. Fax: +44 1509 223187.
E-mail address: H.R.Dullin@lboro.ac.uk (H.R. Dullin).

doi:10.1016/j.physd.2004.12.004

systems with an equilibrium point that loses stability by passing through the $1 : -1$ resonance. This is called the Hamiltonian Hopf bifurcation, and was studied in detail by [14,20,21], also see [2,7].

When the normal form of the corresponding family of Hamiltonians is truncated it becomes Liouville integrable. In this paper, we show that in the integrable normal form of the Hamiltonian Hopf bifurcation the twist vanishes near the bifurcation point. The flow on an invariant 2-dimensional torus is characterised by 2 frequencies. The ratio of these frequencies is the rotation number of the torus. For fixed energy the energy surface is foliated by 2-tori almost everywhere. For a one-parameter family of tori the rotation number is a function of the family parameter. If this rotation function for a family of tori on the energy surface has a critical point we say the twist vanishes for the particular torus at which the critical point occurs. Another, equivalent, way of thinking about this is to consider a Poincaré section transversally to the torus in question and study the resulting mapping of an annulus. In the integrable case, the annulus is foliated by invariant curves. If the rotation number changes from one invariant curve to the next there is twist.

A torus with rational rotation number and twist breaks into a Poincaré–Birkhoff island chain under generic perturbation. At the heart of this chain are an elliptic and a hyperbolic periodic orbit. When the twist vanishes and the rational rotation number is near the critical value (assumed to be a minimum or maximum) the perturbation has a different effect. First of all there are two Poincaré–Birkhoff island chains with periodic orbits of the same period. When the energy (or an external parameter) is changed so that the rational rotation number reaches the extremum these two island chains annihilate in an interesting so called reconnection bifurcation. In this bifurcation, there appear meandering curves, which are invariant curves that are not graphs over the unperturbed invariant curves.

These dynamical consequences of vanishing twist are well known. They were first described by [13], and later studied by [12,4,19]. In [15] and [10], it was shown that the vanishing of twist in one parameter families of maps occurs near the $1 : 3$ resonance. In [9], we have shown that also in 4 dimensional symplectic maps the vanishing of twist appears near resonance. More recently in [8], we have shown that the twist also vanishes near the saddle-centre bifurcation, in which one multiplier passes through zero. In this paper, we show that the principle that the twist vanishes near resonance also applies in the Hamiltonian Hopf bifurcation. For flows, the condition of vanishing twist is one of the conditions for the standard form of the KAM theorem to hold. In this setting, it is usually called the isoenergetic non-degeneracy condition. There exist KAM theorems with weaker conditions [5,18], so that vanishing twist does not necessarily imply that the torus will be destroyed. It does mean, however, that a resonant twistless torus will create all the unexpected dynamics described by the twistless standard map.

In the following two sections, we present well known material about the Hamiltonian Hopf bifurcation, in order to introduce the Hamiltonian and its energy–momentum map and to fix our notation. Then our own contribution starts with the derivation of the actions and the rotation number. The rotation number and its derivative are analysed near critical values of the energy–momentum map, namely near the isolated focus–focus point in the compact case and on the family of relative equilibria. The details of the expansion of the elliptic integrals are given in the Appendix A.

2. Hopf normal form

Consider coordinates $q = (q_1, q_2)$ and conjugate momenta $p = (p_1, p_2)$ so that the symplectic form on $\mathbb{R}^4$ is $\Omega = \mathrm{d}p_1 \wedge \mathrm{d}q_1 + \mathrm{d}p_2 \wedge \mathrm{d}q_2$. The normal form for the Hamiltonian Hopf bifurcation is

$$H(q_1, q_2, p_1, p_2) = \beta\Gamma_1 + \Gamma_2 + \delta(\gamma\Gamma_1 + \Gamma_3) + C\Gamma_1^2 + 2B\Gamma_1\Gamma_3 + 2D\Gamma_3^2 + O_3(\Gamma_1, \Gamma_2, \Gamma_3), \tag{1}$$

where $\Gamma_1 = p_2q_1 - p_1q_2$, $\Gamma_2 = \frac{1}{2}(p_1^2 + p_2^2)$, $\Gamma_3 = \frac{1}{2}(q_1^2 + q_2^2)$, $\Gamma_4 = p_1q_1 + p_2q_2$, and δ is a bifurcation parameter, β, γ, B, C, D are real constants such that $\beta \neq 0$ and $D \neq 0$. The expression O_3 denotes terms of order no less than 3 with respect to Γ_i, $i = 1, 2, 3$. For simplicity we will use the notation $\omega = \beta + \delta\gamma$. The system has an equilibrium point at the origin $p_i = q_i = 0$ with eigenvalues $\sqrt{-\delta} \pm \mathrm{i}\omega$. For ease of notation we write $\alpha = \sqrt{-\delta}$ when $\delta < 0$, so that the eigenvalues of the equilibrium are $\pm\alpha \pm \mathrm{i}\omega$. The dependence of ω on δ is not essential for our purposes, because $\beta \neq 0$. By a symplectic scaling with multiplier the parameter ω can be scaled to 1, and D can be scaled to ± 1 at the same time. We find it useful, however, to keep unscaled variables and parameters until the very last section.

The Hamiltonian system (1) is Liouville integrable when the O_3 terms are omitted. A second independent constant of motion is Γ_1. It generates the S^1 symmetry

$$\Phi : S^1 \times \mathbb{R}^4 \to \mathbb{R}^4,\ \ \Phi(\vartheta, q, p) = (S_\vartheta q, S_\vartheta p), \quad S_\vartheta = \begin{pmatrix} \cos\vartheta & \sin\vartheta \\ -\sin\vartheta & \cos\vartheta \end{pmatrix} \tag{2}$$

The corresponding momentum map $J : \mathbb{R}^4 \to \mathbb{R}$ is given by $J(q, p) = p_2 q_1 - p_1 q_2$, which is Γ_1. Since J generates the periodic flow Φ with period 2π it is an action of the integrable system. We denote the (constant) value of J by j. To perform the reduction with respect to this symmetry we use invariant theory, see e.g. [3]. Singular reduction occurs in this example because the action Φ is not free: the equilibrium (= the origin) is a fixed point of this action. The algebra of polynomials in $\mathbb{R}^4$ that are invariant under Φ is generated by Γ_1, Γ_2, Γ_3 and $\Gamma_4 = p_1 q_1 + p_2 q_2$. This means that any polynomial of q_1, q_2, p_1, p_2 that is invariant under Φ can be written as a polynomial of Γ_i, $i = 1, \ldots, 4$. The generators satisfy the relations

$$G(\Gamma) = \Gamma_1^2/2 + \Gamma_4^2/2 - 2\Gamma_2\Gamma_3 = 0,\ \ \Gamma_2 \geq 0,\ \ \Gamma_3 \geq 0. \tag{3}$$

The reduced phase space $P_j = J^{-1}(j)/S^1$ is defined by (3) with $\Gamma_1 = j$ as a semialgebraic variety in $\mathbb{R}^3$ with coordinates $(\Gamma_2, \Gamma_3, \Gamma_4)$. If $j \neq 0$ the reduced phase space P_j is one sheet of a two-sheeted hyperboloid given by (3), so it is a smooth manifold. But for $j = 0$ it is half of an elliptic cone and hence is not smooth because of the singular point of the cone at the origin $(\Gamma_2, \Gamma_3, \Gamma_4) = (0, 0, 0)$.

The reduced Hamiltonian is

$$H_j(\Gamma_2, \Gamma_3, \Gamma_4) = \omega j + \Gamma_2 + \delta\Gamma_3 + Cj^2 + 2Bj\Gamma_3 + 2D\Gamma_3^2. \tag{4}$$

The surface $H_j^{-1}(h)$ is a parabolic cylinder in $(\Gamma_2, \Gamma_3, \Gamma_4)$ that is independent of Γ_4. The integral curves of the reduced system are given by the intersection of the surface P_j with the surface $H_j^{-1}(h)$, as illustrated in Fig. 1. We denote the intersection by $M_{j,h}$.

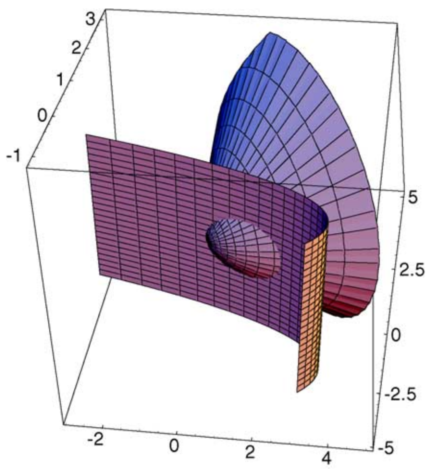

Fig. 1. A typical intersection $M_{j,h}$ of the reduced phase space P_j and the energy surface $H_j^{-1}(h)$.

The Poisson bracket $\{\cdot, \cdot\}$ associated with the standard symplectic structure Ω on $\mathbb{R}^4$ defines a Poisson structure on the algebra of invariant polynomials with brackets

$$\{\Gamma_1, \Gamma_2\} = \{\Gamma_1, \Gamma_3\} = \{\Gamma_1, \Gamma_4\} = 0, \tag{5}$$

$$\{\Gamma_2, \Gamma_3\} = \Gamma_4, \quad \{\Gamma_3, \Gamma_4\} = -2\Gamma_3, \quad \{\Gamma_4, \Gamma_2\} = -2\Gamma_2. \tag{6}$$

The momentum map of the S^1 action used for the reduction induces the Casimir Γ_1 in this Poisson bracket. In addition, also the relation between the generators (3) given by G is a Casimir. Accordingly, the nonzero brackets give a Poisson structure on $\mathbb{R}^3$ with coordinates $(\Gamma_2, \Gamma_3, \Gamma_4)$, that has the reduced spaces P_j as its symplectic leaves. It can be written as

$$\{\Gamma_2, \Gamma_3\} = \partial G/\partial \Gamma_4, \quad \{\Gamma_3, \Gamma_4\} = \partial G/\partial \Gamma_2, \quad \{\Gamma_4, \Gamma_2\} = \partial G/\partial \Gamma_3. \tag{7}$$

The reduced equations of motion are

$$\begin{aligned}
\dot{\Gamma}_2 &= \{\Gamma_2, H_j\} = \Gamma_4 \frac{\partial H_j}{\partial \Gamma_3}, \\
\dot{\Gamma}_3 &= \{\Gamma_3, H_j\} = -\Gamma_4, \\
\dot{\Gamma}_4 &= \{\Gamma_4, H_j\} = -2\Gamma_2 + 2\Gamma_3 \frac{\partial H_j}{\partial \Gamma_3}.
\end{aligned} \tag{8}$$

The integral curves of this flow are given by $M_{j,h}$, the intersection of P_j and $H_j^{-1}(h)$. In general the intersection of these two manifolds is either empty or diffeomorphic to a circle. The preimage of any point in reduced phase space is the set of points in original phase space that are mapped to this point by the momentum map J. If one point in the preimage is known the others can be obtained by letting the flow of J (i.e. the map Φ) act on this point to get the complete fibre. This gives a circle unless starting in the origin. Therefore the preimage of a circle $M_{j,h}$ is a two dimensional torus $\mathbb{T}^2$ in the phase space of the original system.

Exceptions occur for equilibrium points of the reduced system. They occur either when the surface $H_j^{-1}(h)$ is tangent to P_j or when $j = 0$ and $H_0^{-1}(h)$ contains the singular point at the origin (which implies $h = 0$). The preimage of the singular point is not a circle, because $\Gamma_2 = \Gamma_3 = 0$ implies $q_1 = q_2 = p_1 = p_2 = 0$ and this is a fixed point of the flow Φ. This is the equilibrium point in the full system that undergoes the Hopf bifurcation. All other equilibrium points of the recuded system are reconstructed to periodic orbits of the full system; they are relative equilibria of J. The S^1 action generated by J is not free. The origin is a fixed point, and this is the reason why singular reduction is needed in this example.

3. Energy–momentum map

Using the reduced system we can find the critical values of the energy momentum map

$$F : \mathbb{R}^4 \to \mathbb{R}^2, \qquad (p, q) \mapsto F(p, q) = (H(p, q), J(p, q)). \tag{9}$$

The values of the energy–momentum map are denoted by (h, j). For every regular value of F the preimage in phase space is a two dimensional torus. The critical values are determined from equilibrium points of the reduced system because their preimages are not $\mathbb{T}^2$. Since we are interested in a neighbourhood of the origin in phase space for small δ we will only consider a small neighbourhood of the origin in the image of the momentum map.

Consider the reduced equilibrium points caused by the singularity in the reduced space first. This singularity occurs for $j = 0$. The singular point $(\Gamma_2, \Gamma_3, \Gamma_4) = (0, 0, 0)$ has energy $h = 0$. The equilibrium at the origin in phase space is therefore mapped to the origin in the image of the momentum map.

When $\delta > 0$ the intersection $M_{0,0}$ restricted to a neighborhood of the origin in reduced phase space consists only of the origin. It reconstructs to an elliptic equilibrium. However, if $\delta < 0$ then $M_{0,0}$ is a non-smooth circle with a corner, if it is compact. The preimage of $M_{0,0}$ is diffeomorphic to a pinched torus in this case.

Consider next the equilibrium points caused by a tangency of P_j and $H_j^{-1}(h)$. At these critical values of H_j the gradient of H_j and the gradient of G are parallel. Since $\partial G/\partial \Gamma_4 = \Gamma_4$ the tangency may occur only on the hyperplane $\Gamma_4 = 0$. The intersections of P_j and $H_j^{-1}(h)$ with this hyperplane are one branch of a hyperbola and a parabola, respectively. They are described by the equations

$$j^2 = 4\Gamma_2\Gamma_3, \tag{10}$$

$$h = \omega j + Cj^2 + \Gamma_2 - \frac{(\delta + 2Bj)^2}{8D} + 2D\left(\Gamma_3 + \frac{\delta + 2Bj}{4D}\right)^2. \tag{11}$$

At the extremal values of h the two curves are tangent. Eliminating Γ_2 in (10) using (11) gives a polynomial of degree 3 in Γ_3 depending on j and h

$$Q_3(\Gamma_3) := -8D\Gamma_3^3 - 4(\delta + 2Bj)\Gamma_3^2 + 4(h - \omega j - Cj^2)\Gamma_3 - j^2 = 0. \tag{12}$$

This polynomial $Q_3(\Gamma_3)$ gives the value of Γ_4^2 obtained from $G = 0$ and expressed in terms of Γ_3. The tangency between the hyperbola (10) and the parabola (11) occurs when Q_3 has a double root. We will first discuss all values of (h, j) for which a tangency occurs, irrespective of them satisfying the constraints $\Gamma_2 \geq 0$ and $\Gamma_3 \geq 0$. In a second step, the critical values of the energy momentum will be found by consideration of these constraints.

To parametrize all tangencies we make the ansatz $Q_3(z) = -8D(z - d/2)^2(z + s^2/D/2)$ with parameters d and s parametrising the double and single root of Q_3, respectively. This leads to the parametrisation of the tangencies by $s \in \mathbb{R}$. By direct computation, we obtain the basic

Lemma 1. *The discriminant locus of Q_3 that contains the critical values of the energy–momentum map is given by*

$$\begin{aligned} &j_{\mathrm{crit}}(s) = sd(s), \qquad d(s) = \tfrac{\delta - s^2}{2(Bs - D)}, \\ &h_{\mathrm{crit}}(s) = \omega j_{\mathrm{crit}}(s) + Cj_{\mathrm{crit}}(s)^2 - 2d(s)^2 D + 2sj_{\mathrm{crit}}(s). \end{aligned} \tag{13}$$

The root $\Gamma_3 = -s^2/D/2$ always has the opposite sign than D. The curve $(h_{\mathrm{crit}}(s), j_{\mathrm{crit}}(s))$ has singular points when s has one of the singular values satisfying $2Bs^3 - 3s^2D + \delta D = 0$. The number of singular points changes when the discriminant $108\delta D^2(D^2 - \delta B^2)$ vanishes. For small $|\delta|$ the only change occurs at $\delta = 0$, see Fig. 2, for two slices of the "swallowtail".

For $\delta > 0$, the curve has two singular points near the origin for some $s \in (-\sqrt{\delta}, \sqrt{\delta})$. The two singular points are located at

$$\begin{aligned} j^* &= \pm\frac{1}{\sqrt{27}D}\delta^{3/2} + \frac{B}{9D^2}\delta^2 \pm O(\delta^{5/2}) \\ h^* &= \pm\frac{\omega}{\sqrt{27}D}\delta^{3/2} + \frac{2B\omega - 3D}{18D^2}\delta^2 \pm O(\delta^{5/2}) \end{aligned} \tag{14}$$

for small $\delta \geq 0$. The curve of critical values has a self-intersection at $s^2 = \delta$. The intersection point at the origin marks the elliptic equilibrium with eigenvalues $\mathrm{i}(\omega \pm \sqrt{\delta})$. The slopes of the intersecting curves are given by the imaginary parts of the eigenvalues.

For $\delta < 0$, the equilibrium point at the origin is unstable with eigenvalues $\sqrt{-\delta} + \mathrm{i}\omega$. The curve $(j_{\mathrm{crit}}(s), h_{\mathrm{crit}}(s))$ does not intersect the origin, instead the origin is now an isolated critical point. The curve is above the origin for $D < 0$ and below for $D > 0$, e.g. the point on the h-axis with $s = 0$ is at $(j, h) = (0, -\delta^2/8/D)$.

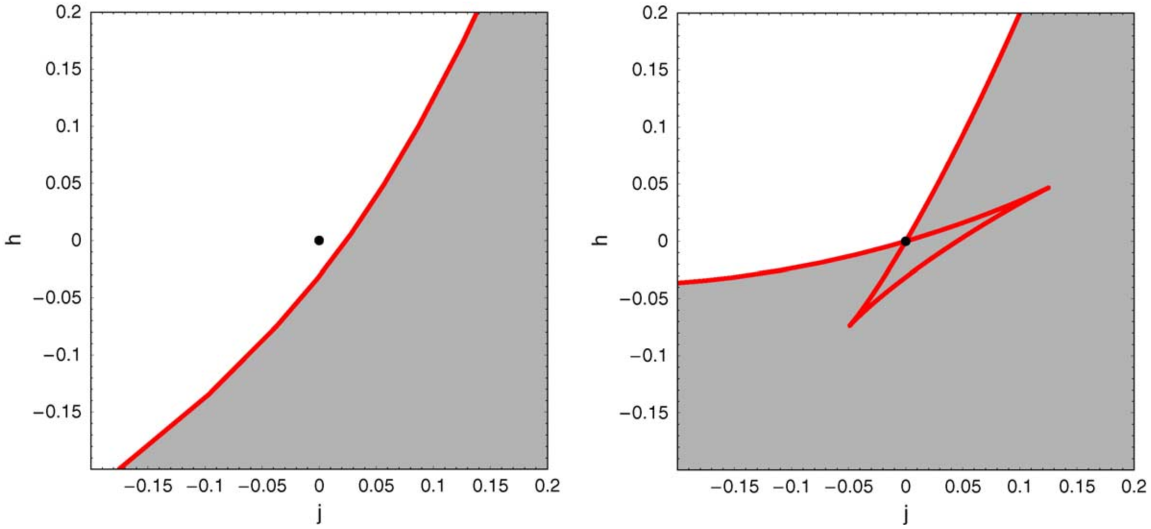

Fig. 2. The discriminant locus of the polynomial Q_3 is the thick (red) line for $\delta = -0.5$ (left) and $\delta = 0.5$ (right). The critical values of the energy–momentum map are contained in the discriminant locus. The white region is the image of the momentum map for $D > 0$. The triangular part for $\delta > 0$ in the right picture is only in the image of the energy–momentum map for $D < 0$. ($B = C = D = \omega = 1.0$).

Only tangencies that occur with the part of the hyperbola in the positive quadrant give critical values of the energy–momentum map since Γ_2 and Γ_3 are both non-negative. The double roots $d(s)$ near $s = 0$ occurs at

$$d(s) = -\frac{\delta}{2D} - O(s). \tag{15}$$

Near the intersection at the origin around $s = \pm\sqrt{\delta}$ the double root is

$$d(s) = \frac{\sqrt{\delta}}{D}(\pm s - \sqrt{\delta}) + O(\pm s - \sqrt{\delta})^2 \tag{16}$$

If $D > 0$ this implies that the smooth curve for $\delta < 0$ is in the (boundary of the) image of the energy–momentum map, while the part of the curve with $s \in (-\sqrt{\delta}, \sqrt{\delta})$ is *not* in the image for $\delta > 0$. Conversely, for $D < 0$ the smooth curve for $\delta < 0$ is not in the image, while for $\delta > 0$ only the triangular part with $s \in [-\sqrt{\delta}, \sqrt{\delta}]$ is in the image. Therefore the union of the bifurcation diagram (i.e. the set of critical values of the energy–momentum map) for $+D$ and $-D$ gives the discrimiant of the polynomial Q_3.

The type of the preimage of the critical values is determined by the character of the intersection $M_{j,h}$. The positive half of the hyperboloid G projects onto the area above the hyperbola given by $j^2 \leq 4\Gamma_2\Gamma_3$. If the parabola (11) touches the boundary of the area from the outside, the preimage in the full phase space is a circle, hence a stable periodic orbit. If the parabola touches from the inside, the preimage is a circle with a separatrix, hence an unstable periodic orbit. This can only occur when $D < 0$, because then the parabola is open upwards. It only occurs when $\delta > 0$ for s between the two singular values enclosing zero. In all other cases the parabola touches from the outside. The complete bifurcation scenario in the two cases therefore is as follows, see Fig. 2 for illustration.

The case $D > 0$: For $\delta < 0$, there is an isolated focus–focus point at the origin and a smooth curve of elliptic periodic orbits nearby. For $\delta > 0$ there is an elliptic equilibirum point at the origin and there are two families of elliptic periodic orbits (non-linear normal modes) emanating from the equilibrium.

The case $D < 0$: For $\delta < 0$, there is nothing but an isolated focus–focus point at the origin. For $\delta > 0$ there is an elliptic equilibirum point at the origin and there are two families of elliptic periodic orbits (non-linear normal modes) emanating from the equilibrium. Both families terminate in cusps formed with the same family of hyperbolic periodic orbits. The set of critical values therefore forms a triangle with two cuspoidal corners and one regular corner at the origin.

4. Actions

From now on we shall assume the parameter D to be a positive number. In this case, each constant energy level is compact and by the Liouville–Arnold theorem it is possible to define action-angle coordinates near regular points of F. To construct the second action we need to integrate the canoncial 1-form Θ over $M_{j,h}$. The differential $\mathrm{d}\Theta$ is the symplectic structure induced from the original symplectic structure Ω by the reduction map on the reduced phase space P_j. To find the form Θ we chose Γ_3 as one variable and find its conjugate variable by solving the partial differential equation

$$\{f(\Gamma_2, \Gamma_3, \Gamma_4), \Gamma_3\} = 1. \tag{17}$$

A solution of (17) is the function

$$f(\Gamma_2, \Gamma_3, \Gamma_4) = \frac{\Gamma_4}{2\Gamma_3}. \tag{18}$$

Then the canonical one form is $\Theta = (\Gamma_4/2\Gamma_3)\mathrm{d}\Gamma_3$ and we obtain

$$J_2(h, j) = \frac{1}{2\pi}\oint_{M_{j,h}} \frac{\Gamma_4 \mathrm{d}\Gamma_3}{2\Gamma_3} = \frac{1}{2\pi}\oint_{M_{j,h}} \frac{\sqrt{4\Gamma_2\Gamma_3 - j^2}}{2\Gamma_3}\mathrm{d}\Gamma_3 \tag{19}$$

for the second action. Here, Γ_4 is considered as a function of Γ_3 by first expressing Γ_4 in terms of Γ_2 and Γ_3 on the reduced phase space P_j and then by expressing Γ_2 in terms of Γ_3 using $H_j = h$. As a result, the polynomial Q_3 is found as already given by (12). This leads to

Theorem 2. *The second action integral in the Hamiltonian Hopf bifurcation normal form with $D > 0$ is defined on the elliptic curve*

$$\mathcal{E} = \{(w, z) : w^2 = Q_3(z)\}. \tag{20}$$

It is explicitly given by the integral of third kind

$$J_2 = \frac{1}{4\pi}\oint \frac{w}{z}\mathrm{d}z. \tag{21}$$

The formula for the action can also be obtained in a classical way, using polar coordinates as in [20]. A slightly different coordinate transformation elucidates the connection between the two approaches. The new symplectic structure is $\Omega = \mathrm{d}P_g \wedge \mathrm{d}g + \mathrm{d}J \wedge \mathrm{d}\phi$ and “symplectic polar coordinates” valid for $q_1^2 + q_2^2 > 0$ are introduced by

$$q_1 = \sqrt{2g}\cos\phi, \qquad p_1 = P_g\sqrt{2g}\cos\phi - J\frac{\sin\phi}{\sqrt{2g}}, \tag{22}$$

$$q_2 = \sqrt{2g}\sin\phi, \qquad p_2 = P_g\sqrt{2g}\sin\phi + J\frac{\cos\phi}{\sqrt{2g}}. \tag{23}$$

The invariant polynomials are related to these coordinates by

$$\Gamma_1 = J, \quad \Gamma_2 = gP_g^2 + \frac{J^2}{4g}, \quad \Gamma_3 = g, \quad \Gamma_4 = 2gP_g. \tag{24}$$

In these variables, the Hamiltonian takes the form

$$H = gP_g^2 + \frac{J^2}{4g} + \omega J + (\delta + 2BJ)g + CJ^2 + 2Dg^2, \tag{25}$$

and the equations of motion are

$$\begin{aligned}\dot{\phi} &= \frac{J}{2g} + \omega + 2Bg + 2CJ,\\ \dot{g} &= 2gP_g,\\ \dot{P}_g &= P_g^2 - \frac{J^2}{4g^2} + (\delta + 2BJ) + 4Dg.\end{aligned} \tag{26}$$

Solving the Hamiltonian (25) for P_g^2 gives

$$P_g^2 = \frac{Q_3(g)}{4g^2} \tag{27}$$

so that the action integral (19) is obtained from integrating the canonical form $P_g \mathrm{d}g$ over a path with constant ϕ.

5. Rotation number

We want to check the isoenergetic non-degeneracy condition of the KAM theorem. A torus is non-degenerate in this sense if the map from the actions to the frequency ratios $\omega_1 : \omega_2$ restricted to a constant energy surface $H = h$ is non-degenerate. This means that the frequency ratio (or rotation number) $W = \omega_1/\omega_2$ changes when the torus is changed at constant energy. On a local transversal Poincaré section this condition is called twist condition.

In our case, this is equivalent to the non-vanishing of the partial derivative of the rotation number W with respect to the action J_1. By definition the winding number is the ratio of frequencies ω_1/ω_2, corresponding to the actions J_1 and J_2. If the Hamiltonian is expressed in terms of J_1 and J_2 then $\partial_1 H(J_1, J_2) = \omega_1$ and $\partial_2 H(J_1, J_2) = \omega_2$. Therefore, we find by implicit differentiation of $J_2(h, j) = j_2$ that

$$W = \frac{\omega_1}{\omega_2} = -\frac{\partial J_2}{\partial j}. \tag{28}$$

However, the simplest way to obtain W is to observe that it is the advance of the angle ϕ conjugate to J during the time of a full period of the motion of $g = \Gamma_3$. The period of the motion is obtained from the reduced equation of motion $\dot{\Gamma}_3 = -\Gamma_4$. On P_j this gives

$$\dot{\Gamma}_3^2 = 4\Gamma_2\Gamma_3 - j^2 \tag{29}$$

and eliminating Γ_2 by using $H_j = h$ gives

$$\left(\frac{\mathrm{d}\Gamma_3}{\mathrm{d}t}\right)^2 = 4\Gamma_3\Gamma_2(\Gamma_3; h, j) - j^2. \tag{30}$$

By separation of variables, we obtain the period of the reduced motion as

$$T(h, j) = \oint \frac{\mathrm{d}\Gamma_3}{\sqrt{4\Gamma_3\Gamma_2 - j^2}} = \oint \frac{\mathrm{d}z}{w}. \tag{31}$$

To obtain the advance of ϕ in time T, we change the time t in (26) to "time" Γ_3 and find

$$\frac{\mathrm{d}\phi}{\mathrm{d}\Gamma_3} = \frac{j + 2\Gamma_3(\omega + 2Cj) + B(2\Gamma_3)^2}{2\Gamma_3\Gamma_4} \tag{32}$$

Expressing Γ_4 in terms of Γ_3 on the reduced phase space P_j as before the period of the solution of this equation gives the rotation number $2\pi W$. The rotation number W can, therefore, be written as a linear combination of integrals of the first, second and third kind,

$$2\pi W(h, j) = (\omega + 2Cj)\oint \frac{\mathrm{d}z}{w} + 2B\oint \frac{z\,\mathrm{d}z}{w} + \frac{j}{2}\oint \frac{\mathrm{d}z}{zw}. \tag{33}$$

The first integral is of the first kind and proportional to the period T. The last integral is of the third kind. When $D > 0$ the polynomial Q_3 has three real roots when (j, h) is in the image of the energy–momentum map. We denote these roots by $z_{\mathrm{neg}}, z_{\mathrm{min}}, z_{\mathrm{max}}$, such that $z_{\mathrm{neg}} \le 0 \le z_{\mathrm{min}} \le z_{\mathrm{max}}$. The closed loop integrals encircle the finite range of positive Q_3, and therefore can be rewritten by the rule

$$\oint = 2\int_{z_{\mathrm{min}}}^{z_{\mathrm{max}}}. \tag{34}$$

The elliptic integrals can be transformed to Legendre standard integrals $K(k)$, $E(k)$, and $\Pi(k)$ of the first, second, and third kind, respectively, with modulus k and characteristic (or parameter) n given by

$$k^2 = \frac{z_{\mathrm{max}} - z_{\mathrm{min}}}{z_{\mathrm{max}} - z_{\mathrm{neg}}}, \qquad n = \frac{z_{\mathrm{max}} - z_{\mathrm{min}}}{z_{\mathrm{max}}}. \tag{35}$$

In this notation we obtain

Theorem 3. *In the Hamiltonian Hopf bifurcation normal form with $D > 0$ the rotation number as a function of (j, h) on the image of the energy–momentum map is given by*

$$W(j, h) = \frac{(2Bz_{\mathrm{neg}} + \omega + 2Cj)K(k) + 2B(z_{\mathrm{max}} - z_{\mathrm{neg}})E(k) + j\Pi(n, k)/(2z_{\mathrm{max}})}{\pi\sqrt{2D}\sqrt{z_{\mathrm{max}} - z_{\mathrm{neg}}}}. \tag{36}$$

Explicit formulas for the vanishing of the twist $\partial W/\partial j = 0$ can be derived from this.

The level lines of the rotation number $W(j, h)$ are shown in Figs. 3 and 4. The function $W(j, h)$ is dynamically relevant only in the image of the energy–momentum part, i.e. not in the grey regions of the figure. Nevertheless, it can be easily analytically continued into this region, and in order to make the spiralling nature of the level lines more obvious we decided to include these non-relevant parts of the contours. In the next section, we will show that these level lines are in fact spirals. Now it is clear that spirals cannot be the level lines of a continuous function. So in fact $W(j, h)$ is locally well defined and smooth for every regular value (j, h), but globally it is not single valued. The particular representation in terms of Legendres complete elliptic integrals contains a branch cut along the positive h-axis, across which W is discontinuous. In this way the spirals are composed of pieces of curves beginning on this cut and ending on the other side of it. The value of W then jumps by one, but the level line smoothly continues across the cut. In order to avoid cluttering of level lines near the origin, the maximal value of W for which level lines are still drawn is 3. This explains the apparent gap in the middle of e.g. the lower right panel for Fig. 3. The spacing of the level lines is 1/10. The details of these pictures will be explained in the next two sections.

The rotation number is a complicated function of the constants of motion (j, h). Near the cases where the discriminant of the elliptic curve E (20) defined by Q_3 vanishes, simpler formulas can be derived. This occurs either at the boundary of the image of the energy–momentum map described by (13), or at the isolated focus–focus point $(h, j) = (0, 0)$ inside the image. In the next section, we will first treat the latter case.

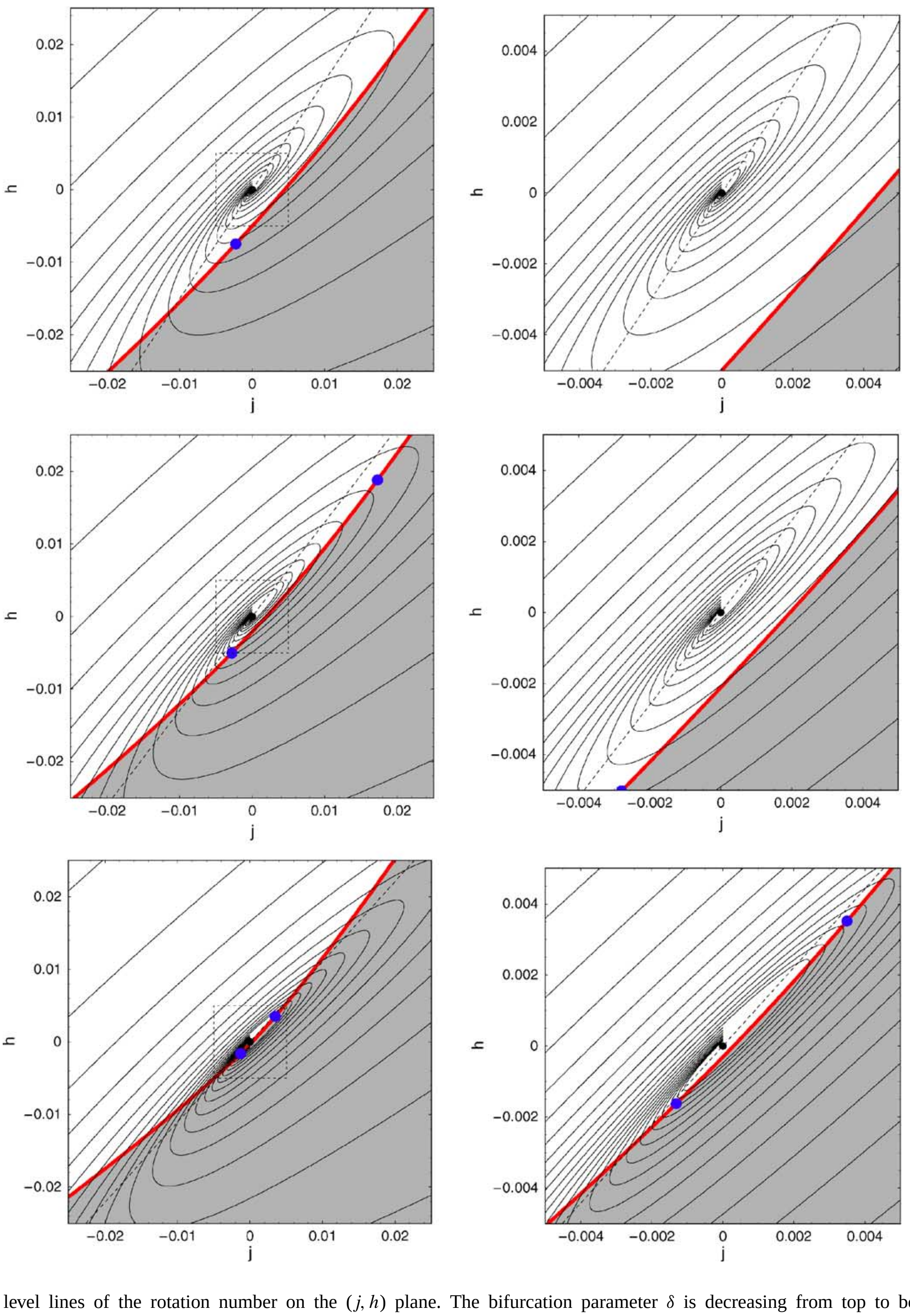

Fig. 3. The level lines of the rotation number on the (j, h) plane. The bifurcation parameter δ is decreasing from top to bottom, $\delta = -0.2, -0.13, -0.05$ ($\omega = B = C = D = 1$). The right panes show zooms of the left ones. The level lines are spirals. The part of the pictures outside the image of the energy–momentum map is grey. The boundary of the image corresponding to a family of relative equilibria is the thick (red) line. The crossing of the curve of vanishing twist with the boundary is indicated by (blue) disks, as given by (51).

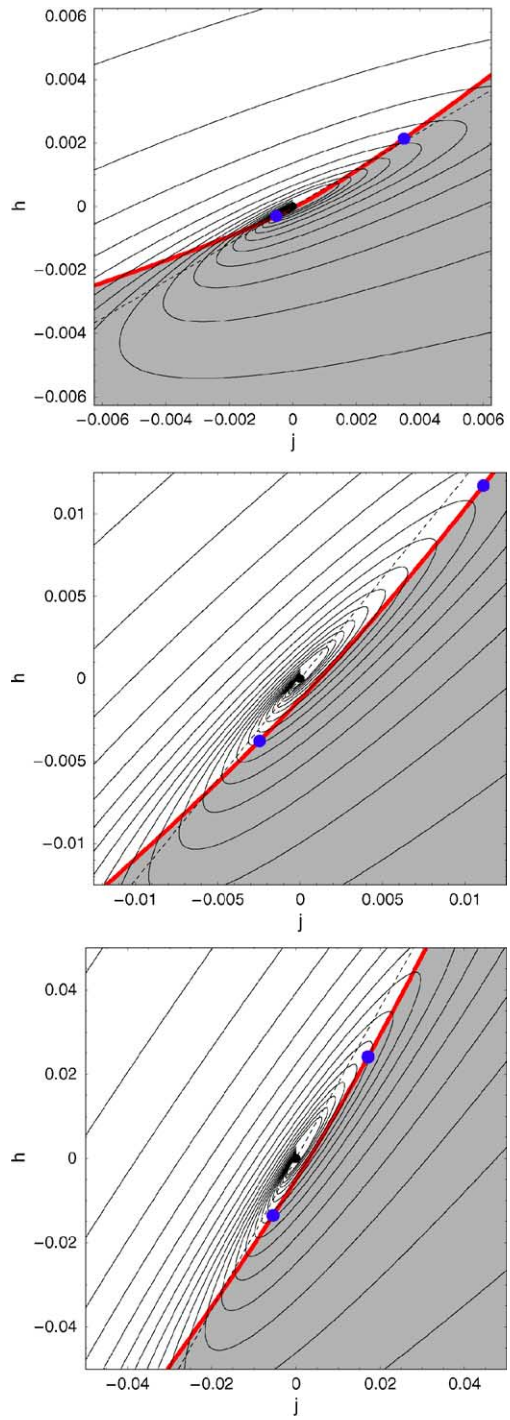

Fig. 4. The level lines of the rotation number on the (j, h) plane. Here, the imaginary part of the eigenvalue ω is changed in addition, from top to bottom $(\delta, \omega) = (-0.02, 1/2), (-0.1, 1), (-0.2, 2)$ $(B = C = D = 1)$. The slope of the tangent of the line of vanishing twist at the origin is shown as a dashed line, as given by (44).

6. Rotation number near the focus–focus point

We introduce a small parameter by scaling h and j by epsilon, hence replace $h \to h\varepsilon$, $j \to j\varepsilon$. This means that we obtain an expansion that approaches the origin on a ray. Alternatively, one can view ε as a formal expansion parameter that keeps track of the fact that both, h and j are small and of the same order. The focus point only exists for $\delta < 0$, which we henceforth assume. At the origin Q_3 reduces to

$$Q_3(z; h = 0, j = 0) = -4z^2(2Dz + \delta), \tag{37}$$

so that $z_{\min}$ and z_{neg} collide at 0 and $z_{\max} = -\delta/2/D$. The roots can be expanded in power series in ε, and the result is

$$\begin{aligned} 2z_{\text{neg}} &= -\frac{l+\rho}{\alpha}\varepsilon + O(\varepsilon^2), \\ 2z_{\min} &= -\frac{l-\rho}{\alpha}\varepsilon + O(\varepsilon^2), \\ 2z_{\max} &= \frac{\alpha^2}{D} + 2\frac{Dl - jB\alpha}{D\alpha}\varepsilon + O(\varepsilon^2). \end{aligned} \tag{38}$$

Here and in the following, we use the abbreviations

$$l = \frac{h - \omega j}{\alpha}, \quad \rho^2 = l^2 + j^2, \quad f = \frac{D}{\alpha^3}, \quad \alpha = \sqrt{-\delta}. \tag{39}$$

The expressions are only real in the case $\delta < 0$, otherwise the focus–focus point does not exist. Inserting this into (35) gives

$$\begin{aligned} k^2 &= 1 - 2f\rho\varepsilon + O(\varepsilon^2), \\ n &= 1 + f(l-\rho)\varepsilon + O(\varepsilon^2). \end{aligned} \tag{40}$$

For small ε both, k and n, are close to 1 and they satisfy the inequality

$$k^2 \le n \le 1. \tag{41}$$

In the limit $k \to 1$, the elliptic integrals are singular, but there are well known expansions that include the logarithmically diverging terms. The details of this expansion can be found in the Appendix A. Thus we have proved

Theorem 4. *The leading order terms of the rotation number $W(j, h)$ near the focus–focus point $(j, h) = 0$ with eigenvalues $\alpha + i\omega$ in the Hamiltonian Hopf bifurcation normal form with $D > 0$ for $\delta < 0$ is*

$$2\pi W(h, j) = -\frac{\omega}{\alpha}\ln\rho - \tan^{-1}\frac{j}{l} + O(1). \tag{42}$$

Keeping terms only up to order 1 is enough because when the twist condition $\partial W/\partial j$ is calculated the present terms both give singular contributions, the constant term disappears and the first order term in ε is very small compared to the singular terms. Note that W is not a single valued function. The fact that $\tan^{-1}(j/l)/2\pi$ changes by one when the origin is encircled is an expression of the monodromy of this focus–focus point, see [7]. From the local expansion derived in the Appendix A one can see that the function is smooth except for a branch cut extending from the origin along the positive h-axis. Here the rotation number jumps by one. The level lines, nevertheless, are globally well defined, except they cannot be labelled by the function values.

The level lines of W are spirals, which are easily parametrized in polar coordinates with the radius ρ as parameter. Instead of viewing these spirals as the level lines of W where W is a many-valued function, it might be easier to see them as the integral curves of a flow in the plane that has an equilibrium point at $h = j = 0$. It can be derived by taking W as a local Hamiltonian. The linear approximation to this flow is best written in complex notation $z = l + \mathrm{i}j$ so that $\dot{z} = -\overline{\lambda z}$ where $\lambda = \alpha + \mathrm{i}\omega$. Therefore, we may formulate the result like this:

Corollary 5. *The level lines of the rotation function* $W(j, h)$ *near the focus–focus critical value* $(0, 0)$ *are the integral curves of a planar node* $\dot{z} = -\lambda\bar{z}$ *where* $\lambda = \alpha + \mathrm{i}\omega$ *is the eigenvalue of the equilibrium point. In particular they are spirals.*

This is in fact true for every simple focus–focus point. For the precise statement of this general result see [11].

Calculating the leading order condition for the vanishing of twist is easily done by differentiating the first two terms of the expansion with respect to j. The result is that

$$\frac{\partial W}{\partial j} = 0 \quad \Rightarrow \quad h(\omega^2 - \alpha^2) = j\omega(\omega^2 + \alpha^2). \tag{43}$$

Thus, we obtain our principal result:

Corollary 6. *The twist vanishes on a line that has a tangent at the focus–focus point* $(j, h) = (0, 0)$ *whose slope is given by*

$$\frac{h}{j} = \omega\frac{\omega^2 + \alpha^2}{\omega^2 - \alpha^2}. \tag{44}$$

Thus, when $\omega > 0$ *for every value of the energy near 0 there is a torus with vanishing twist.*

Notice that this slope only depends on the eigenvalue of the focus–focus point. Approaching the bifurcation point $\alpha \to 0$ the slope approaches ω, see Fig. 4. Further away from the bifurcation the slope may become negative. Again, this corollary is true for any simple focus–focus point with $\omega > 0$, see [11].

7. Vanishing twist of periodic orbits

Now we consider the vanishing of the twist for the relative equilibria $(h_{\mathrm{crit}}(s), j_{\mathrm{crit}}(s))$ in the boundary of the image of the energy–momentum map. First we rescale the parameters, in order to keep the formulas manageable:

$$B = \frac{Db}{\omega},\ C = \frac{Dc}{\omega^2},\ \mu = \frac{\delta}{\omega^2},\ j = \frac{\hat{j}\omega^3}{D},\ h = \frac{\hat{h}\omega^4}{D},\ z = \frac{\zeta\omega^2}{D}. \tag{45}$$

Note that when $\delta < 0$, which is the case we are interested here, we have $\mu = -\alpha^2/\omega^2 < 0$. In terms of the new parameters the polynomial $Q_3(z)$ becomes

$$Q_3(z) = \frac{\omega^6}{D^3}\hat{Q}(\zeta),\ \ \hat{Q}(\zeta) = -(\zeta^3 + (\mu + 2b\hat{j})\zeta^2 + 2(\hat{j} + c\hat{j}^2 - \hat{h})\zeta + \hat{j}^2), \tag{46}$$

and the derivative $\partial W/\partial j$ is

$$\frac{\partial W}{\partial j}(j, h) = \frac{D}{4\pi\omega^3}\left(\oint \frac{(1 + 2c\zeta)\mathrm{d}\zeta}{\zeta\hat{Q}^{1/2}(\zeta)} + \oint \frac{(b\zeta^2 + (1 + 2c\hat{j})\zeta + \hat{j})^2\mathrm{d}\zeta}{\zeta\hat{Q}^{3/2}(\zeta)}\right). \tag{47}$$

The parametrisation of the critical values has already been obtained in (13). After the scaling it reads

$$\hat{d}(s) = \frac{\mu - s^2}{2(bs + 1)}, \quad \hat{j}_{\mathrm{crit}}(s) = s\hat{d}(s), \quad \hat{h}_{\mathrm{crit}} = \omega\hat{j}_{\mathrm{crit}}(s) + c\hat{j}^2_{\mathrm{crit}}(s) + 2\hat{d}(s)^2 + 2s\hat{j}_{\mathrm{crit}}(s). \tag{48}$$

On the curve $(\hat{j}_{\mathrm{crit}}(s), \hat{h}_{\mathrm{crit}}(s))$, the integrals on the right hand side of (47) can be computed by the method of residues. Replacing $\hat{j}$ and $\hat{h}$ wherever they appear by their critical values parametrised by s gives a condition for the vanishing of the twist on the curve of critical values. It implies the following polynomial equation

$$R_9(s) = \sum_{k=0}^{9} a_k s^k = 0, \tag{49}$$

where

$$\begin{aligned}
a_0 &= -12\mu - 4(4+b)\mu^2 - (3b^2 - 16c)\mu^3,\\
a_1 &= -24(5+b)\mu - 4(b+b^2-6c)\mu^2 + 4bc\mu^3,\\
a_2 &= -84 - 12(1+14b+b^2)\mu + 3(15b^2 - 8c + 8bc)\mu^2 - 12c^2\mu^2,\\
a_3 &= 4(30-66b) + 16(b+b^2+9c)\mu + (24b^3 - 52bc)\mu^2,\\
a_4 &= 12(5+25b-23b^2) + (64b^3 - 29b^2 + 192c + 336bc)\mu - 4c(16b^2+15c)\mu^2,\\
a_5 &= -12(8b^3 - 31b^2 - 7b + 14c) - 12b(12b^2 - 29c - 16bc)\mu - 96bc^2\mu^2,\\
a_6 &= 320b^3 + 83b^2 - 312c - 360bc - (96b^4 - 64b^2c - 156c^2)\mu,\\
a_7 &= 4b(32b^3 + 38b^2 - 171c - 48bc) - 64bc(2b^2 - 3c)\mu,\\
a_8 &= 12(8b^4 - 32b^2c - 7c^2),\\
a_9 &= -96bc^2.
\end{aligned} \tag{50}$$

The first two coefficients a_0 and a_1 are of the first order in μ, while a_2 is non-zero for small μ. Therefore, the roots of R_9 can be expanded in powers of $|\mu|^{1/2} = \alpha/\omega$, and for small $|\mu|$ there are only two roots in a $|\mu|^{1/2}$ neighborhood of the origin. The result is

Theorem 7. *The critical values of the twistless relative periodic orbits near the focus–focus point in the Hamiltonian Hopf bifurcation with $D > 0$ are given by the parameter*

$$s_\pm = \pm\sqrt{\frac{-\mu}{7}} + \frac{4}{7^2}(10-b)\mu + O(|\mu|^{3/2}), \tag{51}$$

with corresponding scaled energy–momentum values

$$\hat{j}_\pm = \pm\frac{4}{7}\sqrt{\frac{-\mu^3}{7}} + \frac{8}{7^3}(25-6b)\mu^2 + O(|\mu|^{5/2}), \tag{52}$$

$$\hat{h}_\pm = \pm\frac{4}{7}\sqrt{\frac{-\mu^3}{7}} + \frac{8}{7^3}(43/2-6b)\mu^2 + O(|\mu|^{5/2}). \tag{53}$$

This gives two points shown in the Figs. 3 and 4, at which the curve of vanishing twist emanating from the origin crosses the boundary of the image of the energy–momentum map. The value of the rotation number at these points is

$$\sqrt{5}W_\pm = \frac{1}{2}\sqrt{\frac{7}{-\mu}} \pm \frac{1}{7}(5-2b) + O(|\mu|^{1/2}). \tag{54}$$

We have now treated both limiting cases, that near the focus–focus point, and that near the elliptic relative equilibria. The curve of vanishing twist for all values in between can in principle be computed from the derivative of (36). From our results we conjecture that sufficiently close to the bifurcation the line of twistless tori joins the critical value at (0, 0) with those of the twistless periodic orbits. This is obvious from the pictures presented, but it is very hard to prove rigourously.

8. Conclusion

We have analysed in detail the structure of the rotation number in the normal form of the Hamiltonian Hopf bifurcation for the case $D > 0$ with compact energy surface. The most interesting behaviour can be found for $\delta < 0$, i.e. on the side of the bifurcation where the equilibrium point is unstable, namely a focus–focus point with eigenvalue $\sqrt{-\delta} \pm \mathrm{i}\omega$. In this case, the set of regular values of the energy–momentum map is not simply connected. The boundary of the image corresponds to a family of relative periodic orbits, and in addition there is an isolated critical value corresponding to the unstable focus–focus equilibrium. The rotation number as a function on the image of the energy–momentum map is explicitly given by an elliptic integral. Our main result describes the level lines of the rotation number near the isolated critical value as spirals. Since spirals always have points with a horizontal tangent, the twist vanishes near the focus–focus point. We explicitly computed the tangent to the line of vanishing twist crossing the origin. Moreover, we proved that in the nearby family of relative periodic orbits there are always two periodic orbits with vanishing twist. When the bifurcation is approached these two twistless periodic orbits collide with the unstable equilibrium, rendering it stable on the other side.

Vanishing twist implies that the isoenergetic non-degeneracy condition of the KAM theorem is violated, so that standard results on the persistence of tori cannot be applied. But what is more interesting is that the existence of twistless invariant tori in the Hamiltonian Hopf bifurcation means that after the loss of stability the dynamics is more complicated than expected at first sight. When the neglected higher order terms are put back, the system is in general non-integrable. The perturbation breaks a rational torus with twist into a Poincaré–Birkhoff island chain. However, a rational torus without twist creates a pair of island chains, and when they collide meandering curves appear. These are again invariant tori, but they are not graphs over the original unperturbed torus and carry some amazingly complicated but still regular dynamics. The vanishing of twist near focus–focus points observed here in the setting of the Hamiltonian Hopf bifurcation for the first time is in fact a general phenomenon near focus–focus points and thus lead to the general results presented in [11]. It would be interesting to study the effect of vanishing twist near a focus–focus point in a perturbed, non-integrable model, e.g. in the Hamiltonian Hopf bifurcation.

Acknowledgements

This research is supported by the EPSRC under contract GR/R44911/01. Partial support by the European Research Training Network *Mechanics and Symmetry in Europe* (MASIE), HPRN-CT-2000-00113, is also gratefully acknowledged. AVI was also supported in part by INTAS grant 00-221, RFBI grant 01-01-00335 and RFME grant E00-1-120.

Appendix A. Expansion of *W*

Here, we provide details of the proof of Theorem 4. We need to expand the Legendre standard integrals K, E, and Π in the limit $k \to 1$. For the expansion of the integral of the third kind it is important to take the inequality $k^2 \le n \le 1$ (41) into account. In this limit, the following formulas can e.g. be found in [1]:

$$\Pi(n, k) = K(k) + \frac{1}{2}\pi\mathcal{R}(1 - \Lambda_0(\theta, k)), \tag{55}$$

$$\mathcal{R} = \left(\frac{n}{(1-n)(n-k^2)}\right)^{1/2} = \left(\frac{(z_{\text{neg}} - z_{\text{max}})z_{\text{max}}}{z_{\text{neg}} z_{\text{min}}}\right)^{1/2}. \tag{56}$$

Here, Λ_0 is Heumann's Lambda function, which can be expressed in terms of incomplete elliptic integrals $F(\theta, k)$ and $E(\theta, k)$ of the first and the second kind, respectively, as

$$\Lambda_0(\theta, k) = \frac{2}{\pi}(K(k)E(\theta, k') - (K(k) - E(k))F(\theta, k')), \tag{57}$$

$$\theta = \arcsin\sqrt{\frac{1-n}{1-k^2}} = \arcsin\sqrt{\frac{z_{\text{min}}(z_{\text{max}} - z_{\text{neg}})}{z_{\text{max}}(z_{\text{min}} - z_{\text{neg}})}}. \tag{58}$$

Note that the complementary modulus $k' = \sqrt{1-k^2}$ and the parameter satisfy

$$k'^2 = 1 - k^2 = O(\varepsilon), \quad 1 - n = O(\varepsilon),$$

see (40). Accordingly, k'^2 and $1-n$ are of order ε, while θ is not small but of order 1. The prefactor $\mathcal{R}$ in (55) cancels with the prefactor of Π in (36), up to a factor of 1/2. Therefore, we find the (still exact) formula

$$W = c_1 K + c_2 E + \frac{1}{2}(1 - \Lambda_0(\theta, k)) \tag{59}$$

where with $\sqrt{z_{\text{max}} - z_{\text{neg}}} = \alpha/\sqrt{2D} + O(\varepsilon)$ it follows

$$\pi c_1 = \frac{\omega + 2Bz_{\text{neg}} + 2Cj + j/(2z_{\text{max}})}{\sqrt{2D}\sqrt{z_{\text{max}} - z_{\text{neg}}}} = \frac{\omega}{\alpha} + O(\varepsilon), \tag{60}$$

$$\pi c_2 = \frac{2B\sqrt{z_{\text{max}} - z_{\text{neg}}}}{\sqrt{2D}} = \frac{B\alpha}{D} + O(\varepsilon). \tag{61}$$

The elliptic integral of first kind in the limit $k' \to 0$ has a logarithmic divergence of leading order

$$\Lambda = \log\frac{4}{k'}. \tag{62}$$

The convergent expansions in this limit are

$$K(k) = \Lambda + \frac{\Lambda - 1}{4}k'^2 + O(\Lambda k'^4), \tag{63}$$

$$E(k) = 1 + \frac{1}{2}\left(\Lambda - \frac{1}{2}\right)k'^2 + O(\Lambda k'^4), \tag{64}$$

The incomplete elliptic integrals of modulus k' have regular expansions since $k' \to 0$, so that

$$F(\theta, k') - E(\theta, k') = \int_0^\theta \frac{k'^2 \sin^2\varphi \, d\varphi}{\sqrt{1 - k'^2\sin^2\varphi}} = \left(\frac{\theta}{2} - \frac{\sin 2\theta}{4}\right)k'^2 + O(k'^4), \tag{65}$$

$$F(\theta, k') = \int_0^\theta \frac{d\varphi}{\sqrt{1 - k'^2\sin^2\varphi}} = \theta + \frac{1}{2}\left(\frac{\theta}{2} - \frac{\sin 2\theta}{4}\right)k'^2 + O(k'^4). \tag{66}$$

For the Heumann Lambda function this gives

$$\Lambda_0(\theta, k) = \frac{2}{\pi}\left(\theta + \frac{1}{4}\left(\Lambda - \frac{1}{2}\right)\sin(2\theta)k'^2 + O(\Lambda k'^4)\right). \tag{67}$$

The leading order terms in the expansion of (36) come from the diverging K. Since $E \to 1$ for $k \to 1$ there is only a constant contribution from c_2. From Λ_0 the leading term is merely θ, so that all together

$$\pi W = \frac{\omega}{\alpha}\Lambda + \frac{\pi}{2} - \theta + \frac{B\alpha}{D} + O(\varepsilon) \tag{68}$$

It remains to understand the parameter dependence of θ. Expanding θ gives

$$2\theta \approx 2 \arcsin\sqrt{\frac{\rho - l}{2\rho}} + O(\varepsilon). \tag{69}$$

This can be simplified using the relation

$$2 \arcsin \beta = \arctan \gamma \quad \Rightarrow \quad \gamma = 2\frac{\sqrt{1-\beta^2}\beta}{1-2\beta^2}. \tag{70}$$

Inserting $\beta^2 = (\rho - l)/(2\rho)$ and using $\rho^2 = l^2 + j^2$ gives $\gamma = j/l$, so that (42) is proved. Note that when $j = 0$ we have $\rho = l$ and the root $z_{\min}$ collides with the pole at $z = 0$ in the third kind integral. This is the place where the dependence on the parameters of $\Pi(n, k)$ is not smooth.

References

[1] M. Abramowitz, I.A. Stegun, editors. Handbook of Mathematical Functions with Formulas, Graphs, and Mathematical Tables. Dover Publications Inc., New York, 1992. Reprint of the 1972 edition.

[2] V.I. Arnold, V.V. Kozlov, A.I. Neishtadt, Mathematical aspects of classical and celestial mechanics, Springer-Verlag, Berlin, 1997. Translated from the 1985 Russian original by A. Iacob, Reprint of the original English edition from the series Encyclopaedia of Mathematical Sciences [Dynamical systems. III, Encyclopaedia Math. Sci., 3, Springer, Berlin, 1993; MR 95d:58043a].

[3] R.H. Cushman, L.M. Bates, Global Aspects of Classical Integrable Systems, Birkhäuser Verlag, Basel, 1997.

[4] D. del Castillo-Negrette, J.M. Greene, P.J. Morrison, Area preserving nontwist maps: periodic orbits and transition to chaos, Physica D 91 (1) (1996) 1–23.

[5] A. Delshams, R. de la Llave, KAM theory and a partial justification of Greene's criterion for nontwist maps, SIAM J. Math. Anal. 31 (6) (2000) 1235–1269 (electronic).

[6] J.J. Duistermaat, Bifurcation of periodic solutions near equilibrium points of Hamiltonian systems. In: Bifurcation Theory and Applications (Montecatini, 1983), volume 1057 of Lecture Notes in Math., Springer, Berlin, 1984, pp. 57–105.

[7] J.J. Duistermaat, The monodromy in the Hamiltonian Hopf bifurcation, Z. Angew. Math. Phys. 49 (1) (1998) 156–161.

[8] H.R. Dullin, A.V. Ivanov, (Vanishing) twist in the saddle-centre and period-doubling bifurcation. http://arxiv.org/abs/nlin.CD/0305033, 2003.

[9] H.R. Dullin, J.D. Meiss, Twist singularities for symplectic maps, Chaos 13 (1) (2003) 1–16.

[10] H.R. Dullin, J.D. Meiss, D.G. Sterling, Generic twistless bifurcations, Nonlinearity 13 (2000) 203–224.

[11] H.R. Dullin, S. Vu Ngoc, Vanishing twist near focus–focus points, Nonlinearity 17 (2004) 1777–1786.

[12] J.E. Howard, J. Humpherys, Nonmonotonic twist maps, Physica D 80 (3) (1995) 256–276.

[13] J.E. Howard, S.M. Hohs, Stochasticity and reconnection in hamiltonian systems, Phys. Rev. A 29 (1984) 418.

[14] K.R. Meyer, D. Schmidt, Periodic orbits near L_4 for mass ratios near the critical mass ratio of routh, Cel. Mech. 4 (1971) 99–109.

[15] R. Moeckel, Generic bifurcations of the twist coefficient, Ergodic Theory Dyn. Syst. 10 (1) (1990) 185–195.

[16] J.A. Montaldi, R.M. Roberts, I.N. Stewart, Periodic solutions near equilibria of symmetric Hamiltonian systems, Philos. Trans. R. Soc. Lond. Ser. A 325 (1584) (1988) 237–293.

[17] J. Moser, Periodic orbits near an equilibrium and a theorem by Alan Weinstein, Comm. Pure Appl. Math. 29 (6) (1976) 724–747.

[18] H. Rüssmann. Nondegeneracy in the perturbation theory of integrable dynamical systems. In: Number Theory and Dynamical Systems (York, 1987), volume 134 of London Math. Soc. Lecture Note Ser., Cambridge University Press, Cambridge, 1989, pp. 5–18.
[19] C. Simó, Invariant curves of analytic perturbed nontwist area preserving maps, Regular Chaotic Dyn. 3 (1998) 180–195.
[20] A.G. Sokol'skiĭ, On stability of an autonomous Hamiltonian system with two degrees of freedom under first-order resonance, Prikl. Mat. Meh. 41 (1) (1977) 24–33.
[21] J.-C. van der Meer, The Hamiltonian Hopf bifurcation, volume 1160 of Lecture Notes in Mathematics. Springer-Verlag, Berlin, 1985.
[22] A. Weinstein, Normal modes for nonlinear Hamiltonian systems, Invent. Math. 20 (1973) 47–57.